Physics Letters B 764 (2017) 265–270

Contents lists available at ScienceDirect

Physics Letters B

www.elsevier.com/locate/physletb

Towards saturation of the electron-capture delayed fission probability: The new isotopes ^{240}Es and ^{236}Bk

J. Konki [a], J. Khuyagbaatar [b,c,*], J. Uusitalo [a], P.T. Greenlees [a], K. Auranen [a,1], H. Badran [a], M. Block [b,c,d], R. Briselet [e], D.M. Cox [f,2], M. Dasgupta [g], A. Di Nitto [c,d], Ch.E. Düllmann [b,c,d], T. Grahn [a], K. Hauschild [h], A. Herzán [a,3], R.-D. Herzberg [f], F.P. Heßberger [c], D.J. Hinde [g], R. Julin [a], S. Juutinen [a], E. Jäger [c], B. Kindler [c], J. Krier [c], M. Leino [a], B. Lommel [c], A. Lopez-Martens [h], D.H. Luong [g], M. Mallaburn [i], K. Nishio [j], J. Pakarinen [a], P. Papadakis [a], J. Partanen [a], P. Peura [a,4], P. Rahkila [a], K. Rezynkina [h], P. Ruotsalainen [a], M. Sandzelius [a], J. Sarén [a], C. Scholey [a], J. Sorri [a], S. Stolze [a], B. Sulignano [e], Ch. Theisen [e], A. Ward [f], A. Yakushev [b,c], V. Yakusheva [b,c]

[a] University of Jyvaskyla, Department of Physics, P.O. Box 35, FI-40014 Jyvaskyla, Finland
[b] Helmholtz Institute Mainz, 55099 Mainz, Germany
[c] GSI Helmholtzzentrum für Schwerionenforschung GmbH, 64291 Darmstadt, Germany
[d] Johannes Gutenberg-Universität Mainz, 55099 Mainz, Germany
[e] IRFU, CEA, Université Paris-Saclay, 91191 Gif-sur-Yvette, France
[f] Department of Physics, Oliver Lodge Laboratory, University of Liverpool, Liverpool L69 7ZE, UK
[g] Research School of Physics and Engineering, Australian National University, Canberra, ACT 2601, Australia
[h] CSNSM, Université Paris Sud and CNRS-IN2P3, F-91405 Orsay Campus, France
[i] School of Physics and Astronomy, The University of Manchester, Manchester M13 9PL, UK
[j] Advanced Science Research Center, Japan Atomic Energy Agency, Tokai, Ibaraki 319-1195, Japan

ARTICLE INFO

Article history:
Received 4 October 2016
Received in revised form 9 November 2016
Accepted 21 November 2016
Available online 24 November 2016
Editor: V. Metag

Keywords:
Isotopes with mass 236–240
^{240}Es
^{236}Bk
α decay
Electron-capture delayed fission
Fusion–evaporation reactions

ABSTRACT

The new neutron-deficient nuclei ^{240}Es and ^{236}Bk were synthesised at the gas-filled recoil separator RITU. They were identified by their radioactive decay chains starting from ^{240}Es produced in the fusion–evaporation reaction ^{209}Bi(^{34}S,3n)^{240}Es. Half-lives of 6(2) s and 22^{+13}_{-6} s were obtained for ^{240}Es and ^{236}Bk, respectively. Two groups of α particles with energies $E_\alpha = 8.19(3)$ MeV and 8.09(3) MeV were unambiguously assigned to ^{240}Es. Electron-capture delayed fission branches with probabilities of 0.16(6) and 0.04(2) were measured for ^{240}Es and ^{236}Bk, respectively. These new data show a continuation of the exponential increase of ECDF probabilities in more neutron-deficient isotopes.

1. Introduction

One of the key challenges in understanding the creation and isotopic distribution of elements in nature is knowledge of the stability of the atomic nucleus. A nucleus comprised of Z protons and N neutrons is a complicated quantum bound system that possibly breaks up as a result of the interplay of the different fundamental forces in the interaction between the nucleons. The stability of a nucleus is quantified in terms of the half-life of its radioactive decays such as α, $\beta^{\pm}$, electron capture (EC) and spontaneous fis-

* Corresponding author at: GSI Helmholtzzentrum für Schwerionenforschung GmbH, 64291 Darmstadt, Germany.
E-mail address: J.Khuyagbaatar@gsi.de (J. Khuyagbaatar).
[1] Present address: Physics Division, Argonne National Laboratory, Argonne, IL 60439, USA.
[2] Present address: University of Jyvaskyla, Department of Physics, P.O. Box 35, FI-40014 Jyvaskyla, Finland.
[3] Present address: Department of Physics, Oliver Lodge Laboratory, University of Liverpool, Liverpool L69 7ZE, UK.
[4] Present address: Helsinki Institute of Physics, FI-00014, Helsinki, Finland.

http://dx.doi.org/10.1016/j.physletb.2016.11.038

sion. Experimental data on the radioactive decays of nuclei with different combinations of Z and N has provided a basis for understanding the structure of the atomic nucleus and consequently helped to build up theoretical models [1].

On the other hand, the development and validation of theoretical models is only possible by examining their predictive power in the regions of unstable nuclei with extreme ratios of proton and neutron numbers [1–3]. Therefore, one of the main goals of experimental nuclear physics is to expand our knowledge of previously unknown isotopes where new phenomena can be found and explored as in the case of β and electron-capture delayed fission [4] (βDF and ECDF).

Recently, interest in the delayed fission processes has been renewed due to new studies of the low-energy fission properties of excited nuclei, especially in cases where the ground-state fission of the daughter nucleus is greatly hindered [4]. ECDF (considered in this work) is a two step process. First the mother nucleus undergoes EC decay, which is followed by fission of the excited daughter nucleus. The experimental probability of ECDF (P_{ECDF}) is determined as the ratio of the number of EC decays resulting in fission of the daughter nucleus to the total number of EC decays of the mother nucleus. P_{ECDF} has an exponential dependency on the corresponding fission barrier (B_{sf}) and Q value of the EC decay (Q_{EC}) viz. Q_{EC}-B_{sf}. ECDF has been widely observed in the neutron-deficient odd–odd isotopes of elements Tl–Fr and Np–Md [4]. The ECDF probabilities were found to increase with decreasing neutron number in the isotopic chains and have reached values up to 0.1. The most comprehensive data on ECDF have been collected for Es isotopes with atomic mass numbers $A = 242$–248 [5–7]. The P_{ECDF} increases from $3.5(18) \cdot 10^{-6}$ in ^{248}Es to $6(2) \cdot 10^{-3}$ in ^{242}Es resulting in about one order of magnitude increase in P_{ECDF} for each removal of two neutrons. The trend is expected to continue in the yet unknown more neutron-deficient isotope ^{240}Es.

The synthesis of such exotic nuclei is challenging mainly due to low production rates in the fusion–evaporation reactions that are the preferred way to produce them. Therefore, a dedicated experiment is required for the synthesis and study of each neutron-deficient isotope.

In this letter, we report on the results of experiments where the neutron-deficient isotope ^{240}Es and its daughter ^{236}Bk were synthesised. They have the highest P_{ECDF} measured so far for Es and Bk isotopes.

2. Experimental details

The hitherto unknown neutron-deficient einsteinium isotope ^{240}Es ($Z = 99$ and $N = 141$) was produced as an evaporation residue (ER) of the ^{243}Es* compound nucleus formed in the fusion reaction ^{34}S + ^{209}Bi. The experiment was carried out at the Accelerator Laboratory of the Department of Physics, University of Jyväskylä, Finland. The $^{34}S^{7+}$ ion beam was produced in an ECR ion source and accelerated to energies of 174 MeV and 178 MeV by the K-130 cyclotron. The latter energy was reduced to 175 MeV and 172 MeV for parts of the experiment by using carbon foils with thicknesses of 0.2 and 0.4 mg/cm^2 in front of the target. The $^{209}BiO_2$ target material with a thickness of 0.5 mg/cm^2 (^{209}Bi) was evaporated on to a 0.05 mg/cm^2 carbon-backing foil. The target was rotated to prevent damage due to the irradiation. Typical beam intensity during the experiment was $(0.6$–$1.3) \cdot 10^{12}$ 1/s. The bombarding energies correspond to excitation energies of the ^{243}Es* compound nucleus of 39, 36, 35 and 34 MeV, where the emission of 3 neutrons is predominant (estimated maximum cross section is about 6 nanobarns) according to the calculation of the fusion–evaporation reaction code HIVAP [8].

Evaporation residues recoiling out of the target were separated from the primary beam, target-like and transfer-reaction products according to their predicted magnetic rigidities by the gas-filled recoil separator RITU [9]. The pressure of the helium gas inside the recoil separator was 0.6 mbar and the dipole magnet settings were tuned to yield a magnetic rigidity of 2.0 Tm to guide the ERs to the focal plane.

ERs entering the focal plane detection chamber first passed through a multi-wire proportional counter (MWPC) providing an energy-loss measurement (ΔE) and were then stopped in two adjacent double-sided silicon strip detectors (DSSDs) of the GREAT focal plane spectrometer [10]. In addition, time-of-flight (ToF) between the MWPC and DSSDs was measured. The DSSDs were 300 µm thick and consisted of 60 horizontal and 40 vertical strips with a strip pitch of 1 mm. The DSSDs were surrounded by 28 silicon PIN diodes in a box configuration. Three Clover type [11] high-purity germanium (HPGe) detectors and a planar HPGe detector were used to detect γ rays at the focal plane. In addition, the planar HPGe detector mounted inside the vacuum chamber downstream from the DSSDs was used as a veto detector for the detection of light particles punching through the DSSDs.

The DSSDs were calibrated using the α decays of ^{213,212}Rn, ^{212,211}At and ^{211}Po nuclei produced in transfer reactions during the experiment. The energy resolution (FWHM) of the DSSDs was about 25 keV at an α-particle energy of 8.09 MeV. The vertical strips on the front side of the DSSDs were amplified with high gains in order to have better resolution for α particles while the horizontal strips on the back side were used with lower gains for the detection of high energy events such as fission.

The energies of all signals from the detectors were timestamped with a 100 MHz clock and recorded using the triggerless Total Data Readout (TDR) data-acquisition system [12]. The DSSDs were instrumented with analogue electronics. All of the HPGe and PIN detectors were instrumented with digital Lyrtech VHS-ADC cards. The γ-ray energies were determined using a Moving Window Deconvolution (MWD) algorithm [13] programmed in the FPGA of the 14 bit ADC cards. The temporal and spatial correlations in the data between the detectors were analysed using the GRAIN software package [14].

3. Results

The measured energy spectrum of the events detected in the DSSDs in anticoincidence with the MWPC and the planar HPGe is shown in Fig. 1(a). These events were considered to originate from the α decay of implanted nuclei. Several peaks corresponding to α decays of ^{214m}Fr ($T_{1/2} = 3.35$ ms), ^{214}Fr ($T_{1/2} = 5.0$ ms), ^{213}Rn ($T_{1/2} = 19.5$ ms), ^{212m}At ($T_{1/2} = 119$ ms), ^{212}At ($T_{1/2} = 314$ ms) and ^{211}Po ($T_{1/2} = 516$ ms) were identified in ER–α correlation analysis. Their ERs (hereafter: transfer recoil, TR) were mostly fast (high energy deposit in the DSSDs) and thus also had a short time-of-flight indicating production via transfer reactions. In the further analysis only α-like events detected without correlations with such TRs were included.

In contrast, ERs from fusion reactions have well defined kinematics with smaller kinetic energies and longer time-of-flight which allowed different conditions on the energy and time-of-flight to be applied. The found ER–α correlations with such fusion ERs are shown in Fig. 2 as decay time ($\Delta t_{\mathrm{ER}-\alpha} < 200$ s) versus α-particle energy. The short-lived products from transfer reactions were still observed indicating the presence of a low velocity component of TRs which have the same energy and time-of-flight as the fusion ERs. However, they were distributed in the low-rigidity side of the DSSDs similar to fast TRs. Thus, events with short correlation times (marked as Region 1 in Fig. 2) and from five strips at

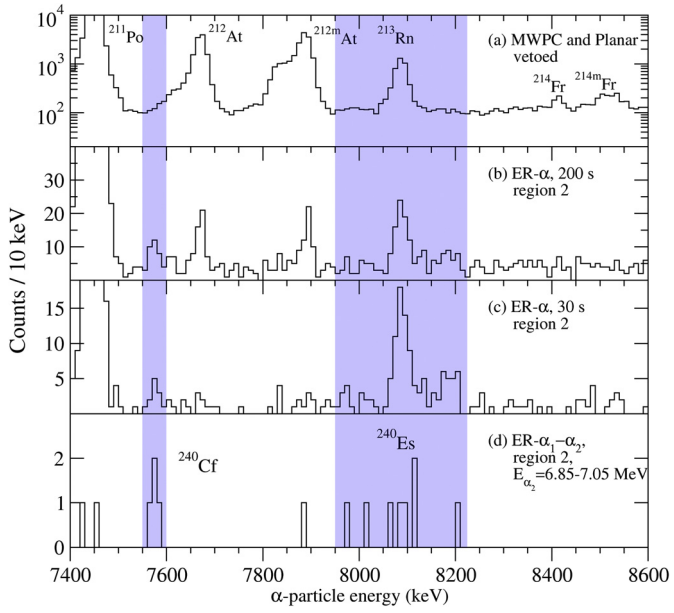

Fig. 1. Energy spectra of α particles measured in the DSSDs and vetoed with the MWPC and the planar HPGe detector from the $^{34}S + ^{209}Bi$ reaction: (a) all α-like events; (b) α-like events following a recoil implantation within 200 s; (c) α-like events following a recoil implantation within 30 s; (d) as in (b) but followed by a second α decay within 1200 s gated on the α particle energy of ^{236}Cm. In panels (b), (c) and (d) the fast components identified as decays from transfer-reaction products shown in Fig. 2 (Region 1) have been excluded (see text for details). The α-particle energy ranges assigned to ^{240}Cf and ^{240}Es are shaded in blue. (For interpretation of the references to colour in this figure legend, the reader is referred to the web version of this article.)

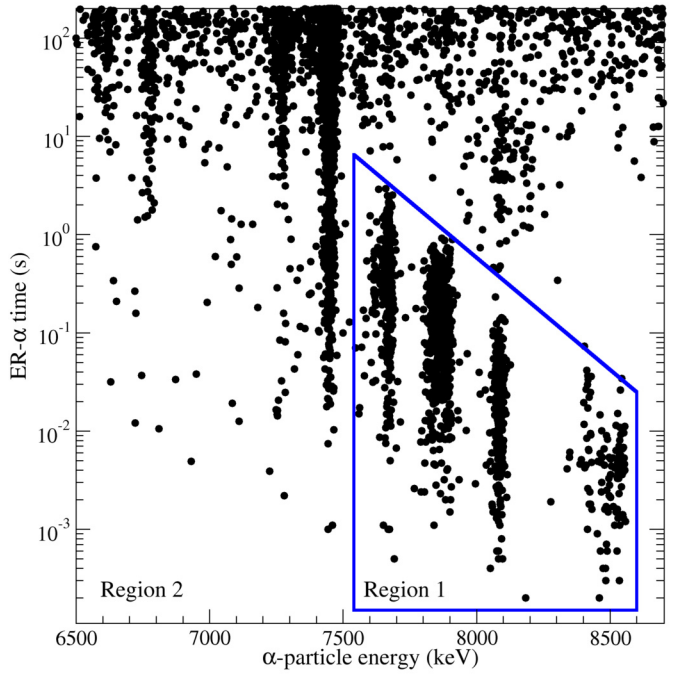

Fig. 2. A two-dimensional plot of the ER–α correlation times on a logarithmic scale as a function of the α-particle energies observed in the $^{34}S + ^{209}Bi$ reaction. The maximum searching time was 200 s.

the end of the low-rigidity side of the DSSDs were removed from further analysis and only the remaining part of the data (labelled Region 2) was inspected for the presence of radioactive decays.

A projection of the two-dimensional plot in Fig. 2 excluding Region 1 is shown in Fig. 1(b) where an additional α line at an energy of 7.57(3) MeV (42 events) has appeared. Choosing a shorter searching time of 30 s reduces the random correlations as shown in Fig. 1(c). Random events corresponding to energies of At have disappeared while at an energy of 8.09(3) MeV (60 events) a peak still remained. Also a well-concentrated peak of α-like events at an energy of 8.19(3) MeV (27 events) is visible.

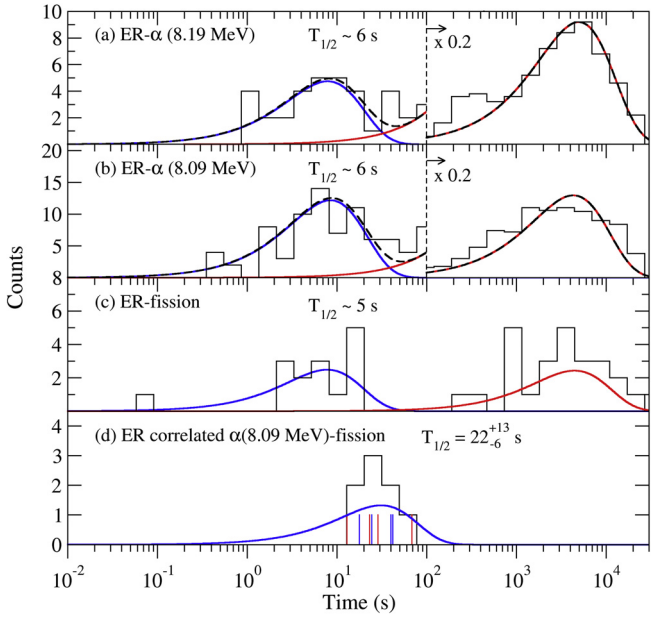

Fig. 3. Time distributions of (a) the correlated α-like events at the energy of 8.19 MeV; (b) 8.09 MeV; (c) the correlated fission-like events without α-like or escape α-like signals between the ER and decay; (d) the fission-like events that were followed after a correlated α at the energy of 8.09 MeV or an escape α-like event. In panels (a) and (b) the blue (red) curve corresponds to the fast (slow) component obtained from a two-component fit to the data. The dashed black line shows the sum of the two components. Note the change in the scale at 100 s. In panels (c) and (d) the half-life of the fission events was determined using the maximum-likelihood method and the time distribution functions with the calculated half-life and the number of events were plotted. In (d) the events where full-energy (escape) α decays were seen are marked with blue (red) lines. See text for details. (For interpretation of the references to colour in this figure legend, the reader is referred to the web version of this article.)

The inspection of time distributions of ER–α(8.19 MeV) and ER–α(8.09 MeV) events show a presence of radioactive decay with a half-life of around 6 s (see Fig. 3(a) and (b)). The correlation search time was expanded to 6 hours to cover distributions of random correlations that have non-negligible contributions to the 6 s-activity. Location of the random peak was in agreement with expected value of ≈ 3700 s deduced from an average counting rate $(2.7 \cdot 10^{-4}$ Hz/pixel) of fusion-like ERs. Hence, half-lives and numbers of events associated with the 6 s-activity were extracted from fits of the whole time distributions by a two-component density distribution functions according to Ref. [15]. A half-life of 6(2) s was deduced for both of the fast activities.

ER–α_1–α_2 correlations were searched for using correlation times of $\Delta t_{ER-\alpha_1} < 200$ s and $\Delta t_{\alpha_1-\alpha_2} < 1200$ s. The resulting two-dimensional α_1–α_2 correlation plot is shown in Fig. 4. Most of the observed events are random correlations corresponding to the high-intensity α peaks of the transfer-reaction products. However, several mother α-decay events that have a non-random origin are followed by α particles of a daughter nucleus with energies in the range 6.85–7.05 MeV. An energy spectrum of these mother α events is shown in Fig. 1(d). Events were detected at energies corresponding to the aforementioned three α lines at 7.57, 8.09 and 8.19 MeV. According to the agreement between the measured $\Delta t_{\alpha_1-\alpha_2(6.95\,\mathrm{MeV})} \approx 430$ s time and literature values, all of these

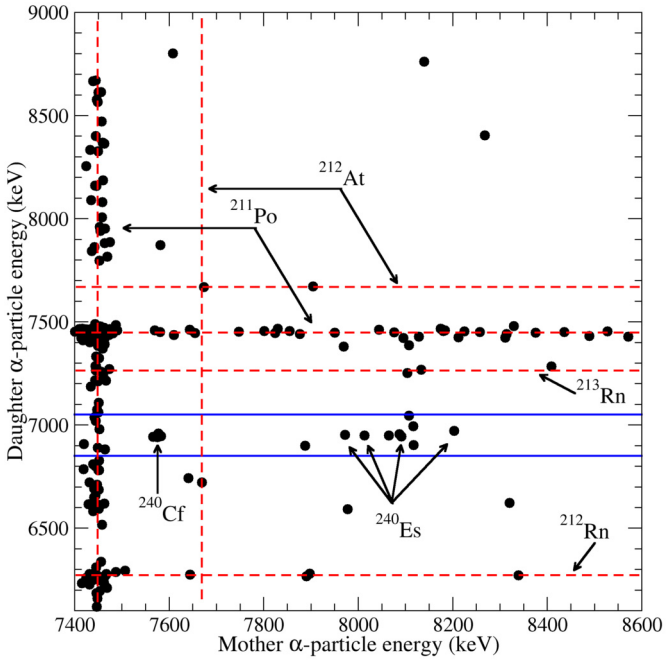

Fig. 4. Mother and daughter α-particle energies for the correlated events of the type ER–α_1–α_2 observed in the $^{34}S + ^{209}Bi$ reaction. The maximum searching times were 200 s for the ER–α_1 pair and 1200 s for the α_1–α_2 pair. Expected random correlations from the decays of transfer-reaction products are marked with dashed red lines. (For interpretation of the references to colour in this figure legend, the reader is referred to the web version of this article.)

chains were attributed to populate ^{236}Cm ($E_\alpha = 6.954(20)$ MeV and $T_{1/2} = 410(50)$ s [16]).

Four of the observed ER–α_1(7.57 MeV)–α_2(^{236}Cm) chains were attributed to the decay of ^{240}Cf. Direct production of ^{240}Cf as ER in the p2n channel of the fusion reaction is estimated to have a cross section of at least ten times smaller than the 3n channel according HIVAP calculations [8] and experimental observations in similar reactions [17]. The contribution of directly produced ^{240}Cf was estimated to be less than one event of ER–α_1(7.57 MeV)–α_2(^{236}Cm) type. Therefore, most of the correlated α-decay events of ^{240}Cf are likely to originate from the EC decay of ^{240}Es considering the statistical uncertainties.

Four chains with $E_{\alpha_1} = 8.09$ MeV and one with $E_{\alpha_1} = 8.19$ MeV were observed. These chains were attributed to originate from the α decay of ^{240}Es, which then proceeds to ^{236}Cm through the EC decay of ^{236}Bk. The observation of such genetic α-decay chains leading to known ^{236}Cm shows that the two unassigned α lines observed in ER–α correlations originate from the decay of ^{240}Es.

We note that two more non-random ER–α_1–α_2 chains were observed with E_{α_1} energies of about 8.02 MeV and 7.97 MeV (see Fig. 1(d) and 4). Additionally, weak peaks were observed in ER–α correlations at these two energies, and half-lives of ≈ 5.2 s and ≈ 4.4 s, respectively, were found for the 8.02(3) MeV and 7.97(3) MeV events (see Fig. 1(c)). Therefore, also these two groups of α particles were tentatively assigned to ^{240}Es. Additionally, following the ER correlated α decays of ^{240}Es, ^{240}Cf and ^{236}Cm, a few correlated decay chains of α(^{232}Pu)–α(^{228}U)–α(^{224}Th)–α(^{220}Ra)–α(^{216}Rn)–α(^{212}Po) were revealed by further event-by-event analysis.

Six photon events with energies of 125(3) keV (three events), 112(3) keV, 89(3) keV and 67(3) keV were detected in prompt coincidence with the correlated 8.09 MeV α particles assigned to ^{240}Es. Two of them have energies similar to $E(K_{\alpha 1}) = 112$ keV, $E(K_{\beta 1}) = 127$ keV and $E(K_{\beta 3}) = 125$ keV X-rays from Bk [18]. However, the tabulated relative intensities of the X-rays are inconsistent

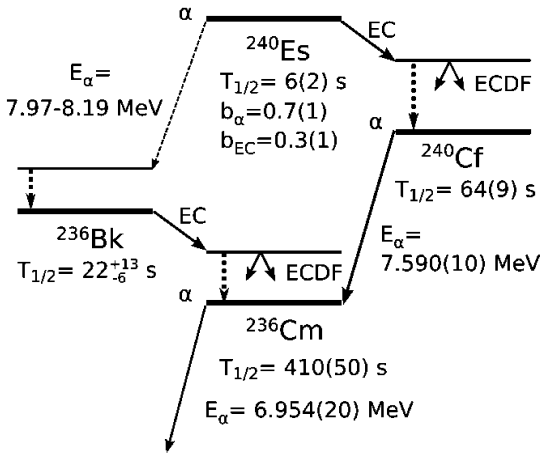

Fig. 5. The proposed decay scheme of the new isotopes ^{240}Es and ^{236}Bk. The measured values for ^{240}Es and ^{236}Bk are from this work, ^{240}Cf from [20] and ^{236}Cm from [16].

with the 125(3) keV events being X-rays. It is possible that the 112(3) keV event is a Bk X-ray, which would support the assignment to the α decay of ^{240}Es. The 125 keV photons are assigned to be γ rays rather than X-rays. The attribution of a 125 keV transition to the proposed decay scheme is still tentative due to the low statistics.

Fission activities were searched for in ER–fission and ER–α–fission correlations. Fission-like events were required to have an energy ≥ 50 MeV (in the DSSD) and no signals in the MWPC. The time distribution of the correlated fission-like events from ER–fission is shown in Fig. 3(c). Again two components similar to the cases of correlated α decays (compare Figs. 3(c) and 3(a), (b)) were observed and the long-lived events were attributed to be random. We noted that γ rays were not detected in coincidence with most of the fission-like events in the random component, whereas, most of the fission-like events in the faster component have at least one γ ray in coincidence.

Fifteen fission-like events with a half-life of 5(2) s were assigned to the decay of ^{240}Es, as a similar half-life was observed for its α decay. However, these fission events are unlikely to originate directly from the ground state of ^{240}Es. Its spontaneous fission branch is greatly hindered due to the unpaired single neutron and proton. Accordingly, these fission events were attributed to occur from the excited states of ^{240}Cf that are populated in the EC decay of ^{240}Es.

Additionally, four ER–α–fission chains were also observed where all ER–α members were 8.09 MeV α events attributed to ^{240}Es. Another four chains were identified as being ER–α(escape)–fission where the α particles escaped in the backward direction from the DSSDs depositing only part of their kinetic energy. The time distribution of the fission events relative to the second decay members is shown in Fig. 3(d). Taking into account the similar time distributions and full-energy detection efficiency of the α particles of the DSSDs, these eight events were attributed to originate from one activity with a half-life of 22^{+13}_{-6} s (Fig. 3(d)). As mentioned above, only α decay of known ^{236}Cm, but not of ^{236}Bk, was followed after the α decay of ^{240}Es, indicating a high EC-decay branch in ^{236}Bk. Therefore, the eight fission members from those chains were attributed to the ECDF decay branch of ^{236}Bk.

4. Discussion and summary

The proposed decay schemes for the new ^{240}Es and ^{236}Bk isotopes are shown in Fig. 5. Branching ratios of $b_\alpha = 0.7(1)$ and

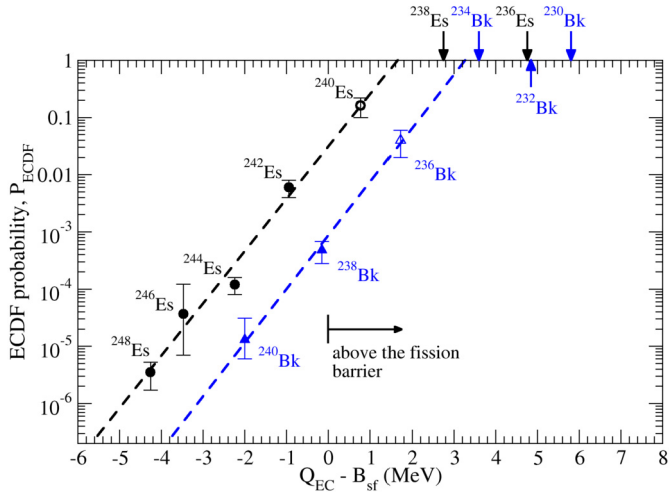

Fig. 6. Electron-capture delayed fission (ECDF) probability (P_{ECDF}) as a function of $Q_{\mathrm{EC}} - B_{\mathrm{sf}}$ of neutron-deficient Es and Bk isotopes. The data points for ^{240}Es and ^{236}Bk are from this work (open symbols). The other P_{ECDF} values (closed symbols) are from [4], Q_{EC} from [19] and B_{sf} from [21].

$b_{\mathrm{EC}} = 0.3(1)$ and a half-life of 6(2) s were deduced for ^{240}Es. The α decays were attributed to feed either the ground state or the excited states in ^{236}Bk. The highest α-particle energy gives $Q_\alpha = 8.33(3)$ MeV that is close to predictions from [19] ($Q_\alpha = 8.17$ MeV), however, due to the often complicated structure of odd–odd nuclei the present data did not allow further assignments of the properties of the states like spins and parities. As mentioned in Section 3, the observed fission events from ER–fission analysis and the ER–α(^{240}Cf) correlations were used to estimate a P_{ECDF} of 0.16(6).

Only an EC-decay branch was identified for ^{236}Bk and a half-life of 22^{+13}_{-6} s was deduced from its ECDF decay branch having a P_{ECDF} of 0.04(2).

The known ECDF probabilities in Es and Bk isotopes together with present new findings are shown in Fig. 6 as a function of the difference of the theoretical Q_{EC} of the mother nucleus [19] and the theoretical fission barrier height B_{sf} of the EC-decay daughter nucleus [21]. Empirical estimates on P_{ECDF} of lighter Es ($A < 242$) and Bk ($A < 238$) isotopes can be given from exponential fit of previously known data for $^{242\text{–}248}$Es and ^{238,240}Bk as function of $Q_{\mathrm{EC}} - B_{\mathrm{sf}}$. Both P_{ECDF} values for ^{240}Es and ^{236}Bk agree well with the trends and confirm a continuation of exponential increase. Positive $Q_{\mathrm{EC}} - B_{\mathrm{sf}}$ values for ^{240}Es and ^{236}Bk would correspond to fission from excited states with energies above barrier heights. However, fission occurs most probably from excited states below the barrier due to the population probabilities of the different excited states in the EC decay. In addition, the absolute values of $Q_{\mathrm{EC}} - B_{\mathrm{sf}}$ are strongly dependent on the particular theoretical calculations and thus their use in detailed discussion is limited.

Nevertheless, the well pronounced systematics of P_{ECDF} as a function of the simple macroscopic variable $Q_{\mathrm{EC}} - B_{\mathrm{sf}}$ are associated with competition between the electromagnetic de-excitation and the penetrability through a fission barrier of the excited nucleus [4]. However, further exponential increase in P_{ECDF} in yet lighter Es and Bk isotopes is not possible because the probability saturates, i.e., $P_{\mathrm{ECDF}} \to 1$. In such cases the fission will dominate over de-excitation of the excited nucleus and the fission barrier may not play a major role anymore. We note that recently, the α-decaying isotope ^{234}Bk was discovered [22] wherein saturated P_{ECDF} is expected according to the exponential fit (see Fig. 6). An evaluation of its P_{ECDF} value has not been possible despite observed fissions [22]. Thus, to date no information on these intriguing P_{ECDF} values exists.

Another important factor in the ECDF process is the fission barrier shape whose influence is not represented explicitly in $Q_{\mathrm{EC}} - B_{\mathrm{sf}}$. The heavy nuclei are known to have multi-humped fission barriers whose heights and shapes strongly affect the penetrability through a total barrier and thus P_{ECDF}. Therefore, the exponential dependence of P_{ECDF} as a function of $Q_{\mathrm{EC}} - B_{\mathrm{sf}}$ should contain information about the shape of the total fission barrier [4,23]. For instance, a relative decrease in P_{ECDF} systematics of Bk isotopes compared to Es can be associated with penetrability through wider barriers in Cm compared to Cf [23].

Experimental cross sections of around a few nanobarns were determined in agreement with calculated ones from the HIVAP code [8]. Despite the reasonably high cross section, identification of the new ^{240}Es and ^{236}Bk isotopes was challenging because of the tail of the random background contributions.

In conclusion, two new neutron-deficient isotopes ^{240}Es and ^{236}Bk isotopes with half-lives of 6(2) s and 22^{+13}_{-6} s, respectively, were identified. The observed α particles with energies of $E_\alpha = 8.19(3)$ MeV and 8.09(3) MeV were unambiguously assigned to the α decay of ^{240}Es. EC decay and ECDF branches were assigned to both isotopes and P_{ECDF} were estimated to be 0.16(6) and 0.04(2) for ^{240}Es and ^{236}Bk, respectively. Our findings extend the systematics of the Es and Bk isotopes where the ECDF probabilities depend exponentially on $Q_{\mathrm{EC}} - B_{\mathrm{sf}}$. No deviations from this trend are observed. This simple dependence that has not yet been fully understood may strongly be affected by the shape of the fission barrier [23]. The experimental data on P_{ECDF} values in more neutron-deficient isotopes of these elements will shed a light on this complex decay process.

Acknowledgements

J. Konki acknowledges support from the Alfred Kordelin Foundation. The use of the GAMMAPOOL loan pool germanium detectors is acknowledged. This work has been supported by the Academy of Finland under the Finnish Centre of Excellence Programme (2012–2017). Support has also been provided by the EU 7th Framework Programme Project No. 262010 (ENSAR). MD, DHL and DJH acknowledge support from the Australian Research Council through grants FL110100098 and DP140100784.

References

[1] L.G.M. Pfützner, M. Karny, K. Riisager, Rev. Mod. Phys. 84 (2012) 567.
[2] O. Sorlin, M.-G. Porquet, Prog. Part. Nucl. Phys. 61 (2008) 602–673.
[3] J. Khuyagbaatar, et al., Phys. Rev. Lett. 115 (2015) 242502.
[4] A.N. Andreyev, et al., Rev. Mod. Phys. 85 (2013) 1541–1559.
[5] D.A. Shaughnessy, et al., Phys. Rev. C 61 (2000) 044609.
[6] D.A. Shaughnessy, et al., Phys. Rev. C 65 (2002) 024612.
[7] D.A. Shaughnessy, et al., Phys. Rev. C 63 (2001) 037603.
[8] W. Reisdorf, Z. Phys. A 300 (1981) 227–238.
[9] M. Leino, et al., Nucl. Instrum. Methods Phys. Res., Sect. B, Beam Interact. Mater. Atoms 99 (1995) 653–656.
[10] R.D. Page, et al., Nucl. Instrum. Methods Phys. Res., Sect. B, Beam Interact. Mater. Atoms 204 (2003) 634–637.
[11] G. Duchêne, et al., Nucl. Instrum. Methods Phys. Res., Sect. A, Accel. Spectrom. Detect. Assoc. Equip. 432 (1999) 90–110.
[12] I.H. Lazarus, et al., IEEE Trans. Nucl. Sci. 48 (2001) 567–569.
[13] A. Georgiev, W. Gast, IEEE Trans. Nucl. Sci. 40 (1993) 770.
[14] P. Rahkila, Nucl. Instrum. Methods Phys. Res., Sect. A, Accel. Spectrom. Detect. Assoc. Equip. 595 (2008) 637–642.
[15] K.-H. Schmidt, et al., Z. Phys. A 316 (1984) 19–26.
[16] J. Khuyagbaatar, et al., Eur. Phys. J. A 46 (2010) 59–67.
[17] J. Khuyagbaatar, et al., Eur. Phys. J. A 37 (2008) 177–183.
[18] R.B. Firestone, et al., Table of Isotopes, 8th edition, John Wiley & Sons, Inc., 1996.

[19] P. Möller, et al., At. Data Nucl. Data Tables 66 (1997) 131–343.
[20] R.J. Silva, et al., Phys. Rev. C 2 (1970) 1948–1951.
[21] P. Möller, et al., Phys. Rev. C 79 (2009) 064304.
[22] D. Kaji, et al., J. Phys. Soc. Jpn. 85 (2016) 015002.
[23] J. Khuyagbaatar, to be published.